

1    **ADSORPTION OF PROPRANOLOL ONTO MONTMORILLONITE:**  
2    **KINETIC, ISOTHERM AND pH STUDIES**

3    María del Mar Orta<sup>1</sup>, Julia Martín<sup>2\*</sup>, Santiago Medina-Carrasco<sup>3</sup>, Juan Luis Santos<sup>2</sup>,  
4    Irene Aparicio<sup>2</sup>, Esteban Alonso<sup>2</sup>

5    *<sup>1</sup>Department of Analytical Chemistry, Faculty of Pharmacy, University of Seville, E-*  
6    *41012 Seville, Spain.*

7    *<sup>2</sup>Department of Analytical Chemistry, Escuela Politécnica Superior, University of*  
8    *Seville. E-41011 Seville, Spain.*

9    *<sup>3</sup>X-Ray Laboratory (CITIUS), University of Seville, E-41012 Seville, Spain.*

10

11

12

13

---

14    Corresponding author: Julia Martín

15    *Address:*

16    Department of Analytical Chemistry, Escuela Politécnica Superior, University of  
17    Seville. C/ Virgen de África, 7, E-41011 Seville, Spain

18    *E-mail:* jbueno@us.es

19    *Phone number:* +34-9-5455-6250

20

21

22

23

24

25

26 **Abstract**

27 The objective of this study was to explore the potential use of the smectite clay mineral  
28 montmorillonite (Mt) as adsorbent in the removal of water containing the emerging  
29 compound propranolol. The Mt was deeply characterized by X-ray diffraction (XRD),  
30 Zeta potential and thermogravimetric analysis (DSC-TG), before and after adsorption  
31 experiments, and their isotherms and kinetic models were fitted to assess the adsorption  
32 of propranolol.

33 The incorporation of propranolol in the interlayer was demonstrated by XRD and DSC-  
34 TG. The results obtained by Zeta potential indicated no adsorption of propranolol in the  
35 surface. Kinetic of propranolol adsorption onto Mt was evaluated using pseudo-first-  
36 order, pseudo-second-order, intra-particle diffusion and Elovich models. Pseudo-second  
37 order was the kinetic model that best described the adsorption of propranolol ( $R^2 >$   
38 0.999). It was possible to obtain a removal efficiency of approximately 96% in less than  
39 1 minute. The adsorption equilibrium isotherm was fitted with the Langmuir,  
40 Freundlich and Dubinin-Radushkevitch mathematical models to obtain the respective  
41 parameters. Freundlich and Dubinin-Radushkevitch were the models that best fitted the  
42 experimental data ( $R^2 >$  0.999). Due to the cationic form of propranolol, the adsorption  
43 by ionic exchange between charged propranolol and sodium cations onto the interlayer  
44 space was the most favorable pathway proposed. Results indicate that adsorption onto  
45 Mt proved to be an efficient method for removing propranolol, thus being a viable  
46 alternative for the treatment of water contaminated with this drug.

47

48 **Keywords:** *Propranolol; Montmorillonite; Adsorption; Water samples*

49

50

## 51 **1. Introduction**

52 Water pollution by pharmaceutically active compounds is increasing in an alarming way  
53 (Basheer et al., 2018; Mompelat et al., 2009). Among various therapeutic groups,  $\beta$ -  
54 blockers are being used worldwide due to the increasing number of patients suffering  
55 from cardiovascular diseases (Ali et al., 2017; Ding et al., 2015). Several of these  
56 medicines, propranolol included, are in the top 200 prescribed medications  
57 (Maszkowska et al., 2014; Huggett et al., 2003). Propranolol is used as a hydrochloride  
58 salt in the treatment of hypertension, pheochromocytoma, angina pectoris, myocardial  
59 infarction and cardiac arrhythmia. It is also used to control hypertrophic  
60 cardiomyopathy, to control symptoms of sympathetic hyperactivity when treating  
61 hyperthyroidism, anxiety disorders, and tremor (Soni, 2014).

62 This drug may originate from hospital effluent, wastewater treatment plants,  
63 pharmaceutical industry waste, and excretion after drug administration to people or  
64 household surplus drugs' disposal (Deblonde et al., 2011). Its widespread use, together  
65 with its often-incomplete metabolism (Maszkowska et al., 2014), means that  
66 propranolol is commonly detected in sewage effluents and surface waters at  
67 concentration levels that range from ng/L to  $\mu$ g/L (Liu et al., 2018; Petrie et al., 2015;  
68 Maszkowska et al., 2014; Lopez-Serna et al., 2013; Santos et al., 2013; Deblonde et al.,  
69 2011). The process used in conventional wastewater treatment plants (WWTP) cannot  
70 remove this compound efficiently (Gao et al., 2018; Gabet-Giraud et al., 2010; Santos et  
71 al., 2013). For example, a study conducted by Santos et al. (2013) in effluent  
72 wastewaters from four different hospitals located in Coimbra (Portugal) showed the  
73 presence of different drugs, among them propranolol, in all hospitals samples analyzed  
74 and also in the WWTP influent and effluent. The removal efficiency for  $\beta$ -blockers  
75 was less than 17%. In another study carried out by Grover et al. (2011), a full-scale

76 granular activated carbon plant treating a WWTP effluent was assessed in terms of  
77 removal efficiency of pharmaceuticals (Grover et al., 2011). Higher removal efficiency  
78 (84–99%) was observed for mebeverine, indomethacine, and diclofenac, while  
79 carbamazepine and propranolol displayed much less removal efficiency (17–23%).  
80 Additionally, due to its characteristic of persistence against natural attenuation, it may  
81 be maintained in the environment for a long period of time (Gao et al., 2018). Some  
82 studies have suggested that propranolol may cause adverse effects on various aquatic  
83 organisms (Ding et al., 2015; Maszkowska et al., 2014; Crane et al., 2006; Falconer et  
84 al., 2006; Fent et al., 2006; Ferrari et al., 2004; Huggett et al., 2002). Propranolol has  
85 the highest acute and chronic toxicity within the class of  $\beta$ -blockers (Maszkowska et al.,  
86 2014; Brausch et al., 2012; Fent et al., 2006; Stanley et al., 2006; Huggett et al., 2002).  
87 In addition, propranolol is also known as an effective antagonist for 5-HT  
88 (hydroxytryptamine) receptor, which is a potential target receptor in wildlife (Alexander  
89 and Wood, 1987). The endocrine-disrupting potential of propranolol on aquatic  
90 organisms was recently emphasized by Massarsky et al. (2011). This is an emerging  
91 issue for the environment, and it can pose a new challenge to water treatment processes.  
92 Several techniques are being studied to treat waters that are contaminated with  
93 pharmaceutically active compounds such as photolysis, photo-Fenton, photocatalysis,  
94 ozonation, nanofiltration and adsorption (Tarpani and Azapagic, 2018; Gao et al., 2018;  
95 Rodríguez-Narváez et al., 2017). Adsorption becomes an interesting alternative for the  
96 treatment of water that is contaminated with pharmaceuticals, since it is versatile, easy  
97 to operate and efficient in removing many pharmaceutical compounds (Singh et al.,  
98 2018). In view of this, the use of natural clays as adsorbents becomes attractive due to  
99 their high capacity to remove a great variety of dissolved organic and inorganic  
100 contaminants and to their large surface area, pore structure and thermal stability, which

101 improves their ability to remove various contaminants from aqueous media (Lozano-  
102 Morales et al., 2018). Montmorillonite (Mt), a smectite clay mineral, has attracted great  
103 interest in the biomedical field because of its high cation exchange capacity, easy  
104 degradation, large specific surface area, low price, easy availability, good adsorption  
105 capacity, and good biocompatibility (Gamba et al., 2015; Jiang et al., 2012). Mt is  
106 widely used in pharmaceutical applications (Farhadnejad et al., 2018; Ullah et al., 2016;  
107 Sánchez Martín et al., 1981). For example, Farhadnejad et al. (2018) designed and  
108 characterized a nanocomposite hydrogel beads, based on carboxymethyl cellulose  
109 (CMC) and Mt-propranolol nanohybrid, for propranolol controlled release. Results  
110 indicated that the Mt-propranolol/CMC nanocomposite beads had high stability against  
111 stomach acid and a sustained- and controlled-release profile for propranolol under the  
112 simulated intestinal conditions. Besides clay minerals, graphene oxide, layered double  
113 hydroxides, mesoporous silica nanocontainers and oxide metallic and metallic  
114 nanoparticles have also evaluated to enhance the mechanical strength and stability of  
115 hydrogel compounds and decrease the drug release rate and burst initial drug release  
116 (Farhadnejad et al., 2018; Kuthati et al., 2015). Furthermore, Mt has also been used as  
117 an adsorbent for the removal of organic pollutants such as pesticides and emerging  
118 pollutants (Martín et al., 2019; Martín et al., 2018; Orta et al., 2018; Gamba et al., 2015;  
119 Marco-Brown et al., 2014; Rauf et al., 2012), heavy metals ions (Barbier et al., 2000) or  
120 organic compounds such as antibiotics (Parolo et al., 2013) from water samples. Mt  
121 adsorbs cationic organic pollutants through ion-exchange processes (Gamba et al.,  
122 2015), while anionic pollutants interact with the positively charged clay edges and  
123 therefore they are only so slightly absorbed; besides, the repulsion that is established  
124 with the negatively charged silicate surface also results in a certain level of desorption

125 (Sannino et al., 1997). To our knowledge, there is no published research regarding the  
126 use of Mt for the removal of  $\beta$ -blockers.

127 The aim of this study was to explore the potential use of Mt as an adsorbent for the  
128 decontamination of water containing the emerging compound propranolol. Mt was  
129 deeply characterized by X-ray diffraction (XRD), Zeta potential and differential  
130 scanning calorimetry and thermogravimetric analysis (DSC-TG), before and after the  
131 adsorption experiments. Their isotherms and kinetic models were fitted to assess the  
132 adsorption of propranolol.

133

## 134 **2. Materials and methods**

### 135 *2.1. Materials and reagents*

136 Mt provided by Castiglioni Pes y Cia, from North Patagonia, Argentina, was used as  
137 receiver. Previous studies had determined its mineralogy and chemical composition  
138 (Magnoli et al., 2008). XRD and chemical analysis indicated that the sample contained  
139 Na Mt (>99%) with quartz and feldspars as minor phases. The structural formula  
140 obtained from the chemical analysis was  $[(\text{Si}_{3.83}\text{Al}_{0.11})(\text{Al}_{1.43}\text{Fe}^{3+}_{0.28}\text{Mg}_{0.30})\text{O}_{10}(\text{OH})_2]$   
141  $\text{Na}_{0.41}$ . The cationic exchange capacity (CEC) determined by the Cu-  
142 triethylenetetramine method (Czímerová et al., 2006) was  $0.8250 \pm 0.0007$  mmol/g of  
143 clay.

144 HPLC-grade, acetonitrile and water were supplied by Romil Ltd. (Barcelona, Spain).

145 Hydrochloric acid, sodium hydroxide and formic acid were obtained from Panreac  
146 (Barcelona, Spain). Ammonium formate was purchased from Sigma-Aldrich  
147 (Steinheim, Germany). All of them were analytical grade.

148 High purity propranolol was purchased from Dr. Ehrenstorfer (Augsburg, Germany).

149 Stock standard solution of propranolol (1000 mg/L) was prepared in methanol and

150 stored at 4°C. Fresh working solutions at different concentration levels were prepared in  
151 deionized water before each experiment.

152

## 153 *2.2. Characterization methods*

154 *X-ray diffraction* patterns were carried out in a Bruker D8 Advance A25 diffractometer  
155 (Bruker, Germany) in Bragg-Brentano configuration. The detector was a Lynxeye PSD  
156 detector (Bruker, Germany) equipped with a copper K  $\alpha$  radiation source (0.15405 nm  
157 wavelength). Step-scan data was taken from 1° to 70°  $2\theta$ , a step width of 0.03°, time  
158 per step of 0.1 s, and tube conditions of 40 kV and 30 mA. The diffractometer was  
159 calibrated mechanically according to the manufacturer's specifications and corundum  
160 standard was used to check the resolution in a wide range of angles.

161 *Zeta potential* was obtained from the mobility of the particles using the Smoluchowski  
162 equation (Smoluchowski, 1941). The Mt, before and after each adsorption experiment,  
163 was suspended in water (1 g/L) and zeta potentials were measured on a Zetasizer  
164 Nanosystem system (Malvern Instruments, Southborough, MA). The pH of the solution  
165 was measured with a Crison GLP 21 pH meter.

166 *Thermal gravimetric analyses* were performed on a Q600 STD (TA instruments, USA).  
167 The samples were heated from 20°C to 900°C at a scanning rate of 10°C/min in a  
168 nitrogen atmosphere.

169 *Liquid Chromatography-tandem mass spectrometry* (LC-MS/MS) analyses were  
170 performed on an Agilent 1200 series HPLC system (Agilent, USA) equipped with a  
171 vacuum degasser, a binary pump, an autosampler and a thermostatic column  
172 compartment. Separation of propranolol was carried out using a HALO C18 (50x4.6  
173 mm i.d.; 2.7  $\mu$ m) analytical column (Teknokroma, Spain) protected by a HALO C18  
174 (5x4.6 mm 1.d.; 2.7  $\mu$ m) guard column (Teknokroma, Spain). Elution was performed by

175 isocratic conditions with acetonitrile (0.1% formic acid) (50%) and a 10 mM aqueous  
176 solution of ammonium formate (0.1% formic acid) (50%), at a flow rate of 0.6 mL min<sup>-1</sup>  
177 with a column temperature of 30°C.

178 A 6410 triple quadrupole (QqQ) mass spectrometer (MS) equipped with an electrospray  
179 ionization source (Agilent, USA) was used for detection. Ionization of analytes was  
180 carried out using the following settings: MS capillary voltage, 3000 V; flow rate of the  
181 drying-gas, 9 L/min; drying-gas temperature, 350°C; and nebulizer pressure was 40 psi.  
182 MassHunter software (Agilent, USA) was used for instrument control and data  
183 acquisition. Compounds were analyzed in multiple reaction monitoring (MRM) mode  
184 and monitored in the positive ionization mode. Two MRM transitions were selected for  
185 each analyte, one was applied for quantification (260 > 116) and another for  
186 confirmation (260 > 56) using a fragmentor of 114 V and an energy collision of 16 eV.

187

### 188 *2.3. Adsorption batch experiments*

189 Batch adsorption experiments of propranolol onto Mt were assessed using a batch  
190 equilibrium method at 25 °C. Solutions with different initial propranolol concentrations  
191 in deionized water (10 mL) containing 20 mg of Mt were added to 20 mL glass bottle  
192 with teflon screw caps. The solutions were stirred at 800 rpm and samples were taken at  
193 different time interval. A pH of approximately 6.5 remained constant during the  
194 adsorption process in all samples. After the contact time, the suspensions were  
195 centrifuged at 8000 rpm during 15 min and supernatants filtered through a 0.22 µm  
196 nylon filter. The final concentrations of propranolol remaining in the aqueous phase  
197 were determined using the LC-MS/MS system.

198 The parameters affecting propranolol adsorption, such as concentration (from 0.5 to 80  
199 mg/L), time (from 0 s to 7 days) and sample pH (from 1 to 12) were evaluated. Each



200 experiment was run in triplicate. The linearity of the method was studied by analyzing  
201 standard solutions in triplicate at concentrations ranging from 0.01  $\mu$  g/mL to 10000  $\mu$   
202 g/mL.

203 The difference in the amount before and after adsorption reveals the amount of adsorbed  
204 propranolol ( $q$ ):

$$205 \quad q = (C_i - C_{eq}) \times \frac{V}{m} \quad (1)$$

206 where V (L) is the volume of the solution, m is the weight of the clay (kg),  $C_i$  (mg/L)  
207 and  $C_{eq}$  (mg/L) are the concentration of the propranolol in the initial and final solution,  
208 respectively. Control experiments were performed without Mt and indicated the  
209 negligible loss of propranolol by volatilization or by adsorption on the glass tubes.

210 The adsorption percentage was calculated as follows:

$$211 \quad \%adsorption = \frac{C_i - C_{eq}}{C_i} \times 100 \quad (2)$$

212 The adsorbent performance was determined by adjustment of the experimental  
213 isotherms to Langmuir, Freundlich and Dubinin-Radushkevitch mathematical model  
214 (Marco-Brown et al., 2014). The Langmuir model is described by the following  
215 equation:

$$216 \quad q = \frac{q_{max} K_L C_e}{1 + (C_e K_L)} \quad (3)$$

217 where,  $q_{max}$  is the maximum amount adsorbed within a monolayer ( $\mu$  mol/g), and  $K_L$  (L/  
218  $\mu$  mol) is the Langmuir dissociation constant, which is related to the adsorption energy.

219 The Freundlich model is described by Equation 4:

$$220 \quad q = K_F C_e^{1/n} \quad (4)$$

221 where  $K_F$  (L/  $\mu$  mol) is the Freundlich constant, which is related to the affinity of the  
 222 adsorbent to the adsorbate, and  $1/n$  is a dimensionless parameter, which indicates how  
 223 adsorption varies as a function of the concentration.

224 The Dubinin-Radushkevitch model is more general than the Langmuir model because  
 225 the former does not assume a homogeneous surface or a constant adsorption potential.

226 This model is described by the following equation:

$$227 \quad q = q_{\max} e^{-K_{DR} \varepsilon^2} \quad (5)$$

228 where  $K_{DR}$  ( $\text{mol}^2/\text{J}^2$ ) is a Dubinin-Radushkevitch constant and  $\varepsilon$  (J/mol) is a Polanyi  
 229 potential, which is related to  $C_e$  by the following equation:

$$230 \quad \varepsilon = RT \ln \left( 1 + \frac{1}{C_e} \right) \quad (6)$$

231 where  $R$  is the gas constant and  $T$  is the temperature in Kelvin.  $K_{DR}$  is related to the  
 232 mean free energy of adsorption per mole of adsorbate ( $E$ , kJ/mol) according to Equation  
 233 7:

$$234 \quad E = (2K_{DR})^{1/2} \quad (7)$$

235 The following mathematical models were employed for the kinetic analysis: pseudo first  
 236 order (PFO), pseudo second order (PSO), intra-particle diffusion (IDM), and Elovich  
 237 models (Equations 8-11, respectively) (Marco-Brown et al., 2014).

$$238 \quad \ln(q_e - q_t) = \ln q_e - k_1 t \quad (8)$$

$$239 \quad \frac{1}{q_t} = \frac{1}{k_2 q_e^2} + \frac{1}{q_e} \quad (9)$$

$$240 \quad q_t = C + k_{id} \sqrt{t} \quad (10)$$

$$241 \quad \frac{dq_t}{dt} = k (q_e - q_t) \quad (11)$$

242 where  $q_e$  and  $q_t$  are the amount of propranolol adsorbed at equilibrium and at time  $t$ ,  
 243 respectively;  $k_1$ ,  $k_2$  and  $k_{id}$  are the rate constants for PFO, PSO, and IDM models,  
 244 respectively.  $C$  is a constant, and  $\alpha$  and  $\beta$  are the Elovich coefficients.

245 To determine the goodness of fit of the model to the experimental data, in addition to  
 246 the value of  $R^2$ , the percentage standard deviation [ $\Delta q$  (%)] was calculated from the  
 247 following equation:

$$248 \quad q(\%) = \sqrt{\frac{\sum \left( \frac{q_t - q_t^{calc}}{q_t} \right)^2}{n - 1}} \cdot 100 \quad (12)$$

249 where  $q_t^{cal}$  is the calculated amount of propranolol adsorbed and  $n$  is the number of  
 250 measurements.

251

### 252 **3. Results and discussion**

#### 253 *3.1. Characterization of Mt and Mt-propranolol*

254 *X-Ray Diffraction:* Precise information about position, intensity, width and shape of  
 255 each individual peak in the diffraction pattern was obtained by Le Bail analysis (Le  
 256 Bail, 2005), using the TOPAS 6 software (Bruker, 2017) (Orta et al., 2018; Martín et  
 257 al., 2018). The values of the goodness of fit (GOF) of the adjustments were checked to  
 258 obtain values close to the unit. At the same time, values of residual factors ( $R_{wp}$  and  
 259  $R_{Bragg}$ ) were obtained. GOF value obtained from the Le Bail fitting for Mt was 2.89, and  
 260  $R_{wp}$  and  $R_{Bragg}$  were 12.14 and 0.916, respectively. These results were small, thus  
 261 indicating coherent data (Young, 1993). The structure used was monoclinic in space  
 262 group C2/m and the lattice parameters were:  $a = 5.12(14) \text{ \AA}$ ,  $b = 9.2(2) \text{ \AA}$ ,  $c = 12.8(3)$   
 263  $\text{ \AA}$ ,  $\beta = 97.4(6)^\circ$ , and  $d = 12.70873 \text{ \AA}$  and  $2\Theta = 6.94985^\circ$  for the (001) plane. After the  
 264 adsorption process of propranolol, GOF,  $R_{wp}$  and  $R_{Bragg}$  were 1.31, 6.03 and 0.377,

265 respectively. The lattice parameters were:  $a = 5.28(3) \text{ \AA}$ ,  $b = 8.71(6) \text{ \AA}$ ,  $c = 13.59(11)$   
266  $\text{ \AA}$ ,  $\beta = 98.3(3)^\circ$ , and  $d = 13.44653 \text{ \AA}$  and  $2\Theta = 6.56809^\circ$ .

267 The Mt presents a monoclinic structure and XRD characterization tests showed a slight  
268 increase from  $12.71 \text{ \AA}$  (Mt) to  $13.45 \text{ \AA}$  (Mt after the adsorption) in the interlayer space  
269 (Figure 1).

270 *Zeta Potential*: The external surface charge of Mt before and after the adsorption assays  
271 was studied at  $\text{pH} \sim 6.5$ . The Zeta potential values were  $-31.1 \pm 1.1 \text{ mV}$  and  $-32.8 \pm 0.9$   
272  $\text{ mV}$ , respectively. These values in the external surface charge of Mt and Mt-propranolol  
273 indicate that there is no adsorption of propranolol in the surface.

274 *Thermal Gravimetric Analyses*: Figure 2 shows the results of DSC (b) and TG (a). The  
275 DSC-TG curves of Mt before adsorption assays show two endothermic peaks around  $90$   
276  $^\circ\text{C}$  and  $680^\circ\text{C}$  associated with the dehydration and dehydroxylation of the clay and with  
277 mass loss of around  $12$  and  $4\%$  respectively (Lapides et al., 2002). The mass loss of the  
278 calcined sample was  $16.59\%$ .

279 After the adsorption of propranolol onto the clay, the endothermic decreases, and there  
280 is a sudden loss of weight, approximately  $9\%$ , due to the dehydration of the water  
281 contained in the interlayer space, which may be due to the propranolol displacing the  
282 water present in the interlayer space. There is a slight loss of around  $9\%$  of weight up to  
283 approximately  $750^\circ\text{C}$ , which may be linked to the degradation of intercalated  
284 propranolol and the loss of structural hydroxyl group. The mass loss of the calcined  
285 sample was  $18.12\%$ .

286

### 287 *3.2. Adsorption of propranolol onto Mt*

288 Experimental data of propranolol adsorption onto Mt loaded samples is shown in Figure  
289 3a as the function of the equilibrium adsorption capacity of propranolol ( $q$ ) versus the

290 equilibrium concentration of propranolol ( $C_e$ ) in the testing solutions. The adsorption  
291 capacity is affected by the initial concentration of solute; lower values of initial  
292 concentration provide greater efficiency in the adsorption process. As we can see from  
293 Figure 3b, adsorption (91-99%) is relatively invariable in the range of 0.5 to 10 mg/L,  
294 while a slight decrease to 81% is observed at 20 mg/L, down to 65% at 80 mg/L. The  
295 adsorption efficiency is higher than the one previously reported for the adsorption of  
296 propranolol onto graphene oxide materials (the greatest adsorption observed was 68%)  
297 (Kyzas et al., 2015).

298 The shape of the isotherm showed L behavior according to Giles' classification (Giles et  
299 al., 1960). The initial curvature here shows that, the more sites in the substrate are filled,  
300 the more difficult it is for a bombarding solute molecule to find a vacant site available.  
301 This also implies that the adsorbed solute molecule is not vertically oriented or that  
302 there is no strong competition from the solvent.

303 In order to estimate whether the adsorption of propranolol in aqueous solution was  
304 favorable or not, different isotherm models were taken into consideration (Langmuir,  
305 Freundlich and Dubinin-Radushkevitch). The fit correlation coefficients ( $R^2$ ) and the  
306 adjustment parameters obtained from each model are shown in Table 1 and plotted in  
307 Figure 4. The Freundlich and Dubinin-Radushkevitch models is more fitting, given the  
308 correlation coefficient values ( $R^2$ ). According to Giles et al. (1960), the analysis of the  
309 term  $1/n$  of Freundlich equation indicates that: when  $n > 1$ , the curve  $q_e$  versus  $C_e$   
310 presents a concave shape with respect to the abscissa axis, and thus the isotherm is  
311 satisfactory to the adsorption; when  $n = 1$ ,  $q_e$  presents a linear shape with variation of  
312  $C_e$ ; when  $n < 1$  the isotherm presents a convex shape with respect to the abscissa axis,  
313 and it is characterized as unfavorable. Since the value of  $n$  obtained in this work is equal  
314 to 1.63, the process is favorable, and as Fig. 3 shows, the isotherm has a concave shape

315 with respect to the abscissa axis. Kyzas et al. (2015) used Freundlich and Langmuir  
316 isotherms to evaluate the propranolol and atenolol adsorption process using graphene  
317 oxide as solid adsorbent. Adsorption isotherms were obtained by varying the initial  
318 concentration of drug (10-150 mg/L) for 24 h and pH 2. Analyzing the Freundlich  
319 isotherm, the authors found an n value of 2.61 and 3.49 for propranolol and atenolol,  
320 respectively, at 25 °C. Haro et al. (2017), in their study of atenolol adsorption in  
321 granular activated carbon (adsorption experiments were performed under variable  
322 atenolol concentrations (5-900 mg/L), adsorbent 10 g/L, pH 6.0), also found that the  
323 model that fitted best the experimental data was the Freundlich model, and the value of  
324 parameter n that they found was 2.4 (mg/g).

325 Regarding the Dubinin-Radushkevitch model, the free energy E of adsorption (kJ/mol)  
326 with Eq. (7) provides information on the adsorption mechanism. If  $E < 8$  kJ/mol, the  
327 adsorption process follows a molecular interactional mechanism preferentially, while  
328 for  $E > 8$  kJ/mol ion-exchange is envisaged. E values showed in Table 1 could indicate  
329 that an ionic exchange between charged propranolol and sodium cations in the free sites  
330 of Mt could be the dominant adsorption mechanism.

331

### 332 *3.3. Adsorption kinetics*

333 The kinetic behavior of Mt was examined. The experiments were made using a  
334 propranolol solution at  $C_i = 10$  mg/L. Figure 5 shows the kinetic data obtained. The  
335 most impressive piece of the kinetic data is that, in the first minute, propranolol  
336 molecules were removed by ~96%, which is an extremely rapid kinetic behavior.  
337 Afterwards, propranolol remained retained into the material for at least seven days after  
338 the assay. When submitting these data to a statistical analysis, it can be observed that  
339 between 5, 10, 30 and 60 min there was not a significant difference between the % of

340 adsorption ( $p= 0.05$ ). Therefore, Mt required shorter equilibrium times compared to  
341 other adsorbents. For example, 24 h were needed to reach a removal of propranolol of  
342 97% from water samples using synthetic mica Na-mica-4 or of 50% using C<sub>18</sub>-mica-4  
343 (Martín et al., 2018). Haro et al. (2017) and Kyzas et al. (2015) evaluated the removal of  
344  $\beta$ -blockers in aqueous solutions through adsorption process using granular activated  
345 carbon as solid adsorbent and it was possible to reach a removal efficiency of  
346 approximately 88% after 90 min and 68% after 180 min for atenolol and propranolol,  
347 respectively. Recently, Ali et al. (2017) reported the sorption of propranolol on ionic  
348 liquid iron new generation adsorbent. The maximum removal of propranolol was 90%  
349 with varying times: 40 min, pH: 9.0, initial concentration 50  $\mu$  g/L; Dose: 1.0 g/L. The  
350 ionic liquid iron nanocomposite adsorbent was selective for propranolol.

351 In order to examine the rate-controlling mechanism of the adsorption process, the PFO,  
352 PSO, IDM and Elovich models were evaluated to fit the experimental data. The values  
353 of the kinetic parameters, calculated  $q_e$ , determination coefficient ( $R^2$ ) and the  
354 experimental error ( $\Delta q$  (%), chi-square error) are shown in Table 2. Data obtained from  
355 kinetic studies for both materials fit the PSO model better than the other models ( $R^2 >$   
356 0.999). This result was expected since this model predicts that the adsorbate removal  
357 rate as a function of time is directly proportional to the difference between the adsorbed  
358 amount at equilibrium and the amount adsorbed at any time. Therefore, this model  
359 typically does not fit throughout the whole of the time range, only during the initial  
360 minutes of the adsorption process (Ho and Mckay, 1999). The kinetic curve is  
361 considered to be a classical example of kinetic adsorption plot, in which the pollutant's  
362 removal is very fast during the first minutes of contact. This kinetic behavior is common  
363 in adsorption of different pollutants onto polymeric adsorbents (Kyzas et al., 2015; Haro  
364 et al., 2017).

365

### 366 *3.4. Influence of the pH on the propranolol adsorption*

367 One of the most important factors which influence the adsorption behavior of any  
368 adsorbent material is the pH of the solution. The adsorption of propranolol onto Mt as a  
369 function of pH was investigated for pH values ranging from 1 to 12 with an initial  
370 concentration of propranolol of 10 mg/L (Figure 6). The results show that the amount  
371 adsorbed was independent of the pH of the solution between 2-9 (% adsorption > 94%).  
372 Propranolol is a secondary amine with constant acidity (pKa) equal to 9.5 and thus the  
373 species of the  $\beta$ -blocker present in solution at pHs ranging from 2 to 9 are mainly  
374 positively charged. This phenomenon favors the adsorption process on Mt where the  
375 main reaction that must take place is the exchange of the sodium ions of Mt with those  
376 of the propranolol-ammonium ions of the solution. At very low pH (1) values, the  
377 adsorption slightly decreased to 86%, which could indicate some substitution of sodium  
378 by hydrogen ions. At pH > 9, the amine is released by hydrolysis and is precipitated  
379 because of its low solubility, therefore impeding the study of adsorption at pH 12. This  
380 same issue was observed by Sánchez Martín et al. (1981) when studying the interaction  
381 of Mt with a constant release of propranolol.

382

383

### 384 **4. Conclusions**

385 The natural phyllosilicate Mt proved to be a suitable adsorbent for the elimination of the  
386  $\beta$ -blocker propranolol, being a viable alternative for the treatment of water  
387 contaminated with this drug. According to the results, this adsorbent required shorter  
388 equilibrium times compared with other adsorbents, reaching 96% adsorption in less than  
389 one minute. It was observed that propranolol adsorption kinetics onto Mt followed the



390 PSO model. The adsorption capacity obtained depended on the initial concentration of  
391 solute; lower values of initial concentration provided greater efficiency in the adsorption  
392 process. Propranolol adsorption onto Mt was well described by the Freundlich and  
393 Dubinin-Radushkevitch models ( $R^2 > 0.993$ ), being the ionic exchange between charged  
394 propranolol and inorganic cations in the free sites the most favorable pathway.  
395 Additionally, the variable pH presented a low influence in the range of 1 to 9.  
396 XRD, DSC-TG and potential Z were used in order to confirm the entrance of  
397 propranolol onto Mt. The XRD showed a slight increase in the interlayer space after the  
398 adsorption, suggesting that the retention of propranolol occurs in the interlayer space.  
399 The results of the DSC-TG also corroborated the adsorption. While the results obtained  
400 by Zeta potential indicated no adsorption of propranolol in the surface.  
401 Studies like this one prove the potential of certain adsorbent materials for their use in  
402 the industrial treatment of waters affected by different types of pollutants. Obtaining  
403 universal materials, with a high elimination yield and that can be applied to a wide  
404 range of contaminants, is the main challenge in this field. Therefore, the following steps  
405 in this line of research would be: evaluating how these materials eliminate other  
406 families of water contaminants, their application on an industrial scale and, in parallel,  
407 improving the functionality of the material itself. On the other hand, its use in cleaning  
408 and preconcentration stages in analytical processes is also plausible according to some  
409 of the interesting properties of the materials tested.

410

#### 411 **Acknowledgements**

412 This work was supported by the Spanish Ministry of Economy, Industry and  
413 Competitiveness (Project No. CTM2017-82778-R) and by the University of Seville,  
414 through its *VI Plan Propio de Investigación*. The authors are grateful to the X-ray

415 Laboratory and Functional Characterization Services of the *Centro de Investigación*  
416 *Tecnología e Innovación de la Universidad de Sevilla* (CITIUS).

417

## 418 **References**

419 Alexander, B.S., Wood, M.D., 1987. Stereoselective blockade of central [3H] 5-  
420 hydroxytryptamine binding to multiple sites (5-HT1A, 5-HT1B and 5-HT1C) by  
421 mianserin and propranolol. *J. Pharm. Pharmacol.* 39, 664–666.

422 Ali, I., Alothman, Z.A., Alwarthan, A., 2017. Uptake of propranolol on ionic liquid iron  
423 nanocomposite adsorbent: kinetic, thermodynamics and mechanism of adsorption.  
424 *J. Mol. Liq.* 236, 205–213.

425 Barbier, F., Duc, G., Petit-Ramel, M., 2000. Adsorption of lead and cadmium ions from  
426 aqueous solution to the montmorillonite/water interface, *Colloids Surf. A* 166,  
427 153–159.

428 Basheer, A.A., 2018. New generation nano-adsorbents for the removal of emerging  
429 contaminants in water, *J. Mol. Liq.* 261, 583–593.

430 Brausch, J.M., Connors, K.A., Brooks, B.W., Rand, G.M., 2012. Reviews of Environ-  
431 mental Contamination and Toxicology. Human Pharmaceuticals in the Aquatic  
432 Environment: a Review of Recent Toxicological Studies and Considerations for  
433 Toxicity Testing, vol. 218. Springer, pp. 1–99.

434 Bruker, 2017. Bruker AXS GmbH, Karlsruhe, Germany Search PubMed.

435 Crane, M., Watts, C., Boucard, T., 2006. Chronic aquatic environmental risks from  
436 exposure to human pharmaceuticals, *Sci. Total Environ.* 367, 23–41.

437 Czimerová, A., Bujdák, J., Dohrmann, R., 2006. Traditional and novel methods for  
438 estimating the layer charge of smectites. *Appl. Clay Sci.* 34, 2–13.

439 Deblonde, T., Cossu-Leguille, C., Hartemann, P., 2011. Emerging pollutants in  
440 wastewater: a review of the literature. *Int. J. Hyg Environ. Health* 214, 442-448.

441 Ding, J., Lu, G., Li, G., Nie, Y., Liu, J., 2015. Biological fate and effects  
442 of propranolol in an experimental aquatic food chain. *Sci. Total Environ.* 532, 31-  
443 39.

444 Falconer, I.R., Chapman, H.F., Moore, M.R., Ranmuthugala, G., 2006. Endocrine-  
445 disrupting compounds: a review of their challenge to sustainable and safe water  
446 supply and water reuse, *Environ. Toxicol.* 21, 181–191.

447 Farhadnejad, H., Mortazavi, S.A., Erfan, M., Darbasizadeh, B., Motasadizadeh, H.,  
448 Fatahi, Y., 2018. Facile preparation and characterization of pH sensitive Mt/CMC  
449 nanocomposite hydrogel beads for propranolol controlled release. *Int. J. Biol.*  
450 *Macromol.* 111, 696–705.

451 Fent, K., Weston, A.A., Caminada, D., 2006. Ecotoxicology of human pharmaceuticals.  
452 *Aquat. Toxicol.* 76, 122-159.

453 Ferrari, B., Mons, R., Vollat, B., Fraysse, B., Paxeus, N.A., 2004. Environmental risk  
454 assessment of six human pharmaceuticals: are the current environmental risk  
455 assessment procedures sufficient for the protection of the aquatic environment?  
456 *Environ. Toxicol. Chem.* 23, 1344–1354.

457 Gabet-Giraud, V., Miege, C., Choubert, J.M., Matin Ruel, S., Coquery, M., 2010.  
458 Occurrence and removal of estrogens and beta blockers by various processes in  
459 wastewater treatment plants. *Sci. Total Environ.* 408, 4257-4269.

460 Gamba, M., Flores, F.M., Madejová, J., Sánchez, R.M.T., 2015. Comparison of imazalil  
461 removal onto montmorillonite and nanomontmorillonite and adsorption surface  
462 sites involved: An approach for agricultural wastewater treatment. *Ind. Eng.*  
463 *Chem. Res.* 54 (5), 1529-1538.

464 Gao, Y.q., Gao, N.y., Yin, D.q., Tian, F.x., Zheng Q.f., 2018. Oxidation of the b-blocker  
465 propranolol by UV/persulfate: Effect, mechanism and toxicity investigation.  
466 Chemosphere 201, 50-58.

467 Giles, C.H., Macewan, T.H., Nakhwa, S.N., Smith, D.J., 1960. Studies in adsorption.  
468 Part XI. A system of classification of solution adsorption isotherms, and its use in  
469 diagnosis of adsorption mechanisms and in measurement of specific surface areas  
470 of solids. J. Chem. Soc. 786, 3973–3993.

471 Grover, D.P., Zhou, J.L., Frickers, P.E., Readman, J.W., 2011. Improved removal of  
472 estrogenic and pharmaceutical compounds in sewage effluent by full scale  
473 granular activated carbon: impact on receiving river water. J. Hazard. Mater. 185,  
474 1005–1011.

475 Haro, N.K., Del Vecchio, P., Marcilio, N.R., Feris, L.A., 2017. Removal of atenolol by  
476 adsorption e Study of kinetics and equilibrium. J. Cleaner Product. 154, 214–219.

477 Ho, Y.S., McKay, G., 1999. Pseudo-second order model for sorption processes. Process  
478 Biochem, 34, 451–465.

479 Huggett, D.B., Brooks, B.W., Peterson, B., Foran, C.M., Schlenk, D., 2002. Toxicity  
480 of selected beta-adrenergic receptor-blocking pharmaceuticals on aquatic  
481 organisms. Arch. Environ. Contam. Toxicol. 23, 229–235.

482 Huggett, D.B., Khan, I., Foran, C.M., Schlenk, D., 2003. Determination of beta-  
483 adrenergic receptor blocking pharmaceuticals in United States wastewater  
484 effluent. Environ. Pollut. 121(2), 199–205.

485 Jiang, J.Q., Ashekuzzaman, S.M., 2012. Development of novel inorganic adsorbent for  
486 water treatment. Curr. Op. Chem. Eng. 1, 191–199.

487 Kuthati, Y., Kankala, R.K., Lee, C-H., 2015. Layered double hydroxide nanoparticles  
488 for biomedical applications: Current status and recent prospects. *Appl. Clay Sci.*  
489 112–113, 100–116.

490 Kyzas, G.Z., Koltsakidou, A., Nanaki, S.G., Bikiaris, D.N., Lambropoulou, D.A., 2015.  
491 Removal of beta-blockers from aqueous media by adsorption onto graphene  
492 oxide. *Sci.Total Environ.* 537, 411–420.

493 Lapides, I., Yariv, S., Golodnitsky, D., 2002. Simultaneous DTA-TG Study of  
494 Montmorillonite Mechanochemically Treated with Crystal-violet. *J. Therm.*  
495 *Anal. Cal.* 67, 99–112.

496 Le Bail, A., 2005. Whole powder pattern decomposition methods and applications: a  
497 retrospection. *Powder Diffr.* 20, 316.

498 Liu, J., Dan, X., Lu, G., Shena, J., Wua, D., Yana, Z., 2018. Investigation of  
499 pharmaceutically active compounds in an urban receiving water: Occurrence, fate  
500 and environmental risk assessment. *Ecotoxicol. Environ. Saf.* 154, 214–220.

501 Lopez-Serna, R., Jurado, A., Vázquez-Suñe, E., Carrera, J., Petrovic, M., Barcelo, D.,  
502 2013. Occurrence of 95 pharmaceuticals and transformation products in urban  
503 groundwaters underlying the metropolis of Barcelona. Spain. *Environ. Pollut.*  
504 174, 305-315.

505 Lozano-Morales, V., Gardi, I., Nir, S., Undabeytia, T., 2018.  
506 Removal of pharmaceuticals from water by clay-cationic starch sorbents. *J. Clean.*  
507 *Product.* 190,703-711.

508 Magnoli, A. P., Tallone, L., Rosa, C.A.R., Dalcero, A.M., Chiacchiera, S.M., Torres  
509 Sanchez, R.M., 2008. Commercial bentonites as detoxifier of broiler feed  
510 contaminated with aflatoxin. *Appl. Clay Sci.* 40, 63–71.

511 Marco-Brown, J.L., Areco, M.M., Torres Sánchez, R.M., dos Santos Afonso, M., 2014.  
512 Adsorption of picloram herbicide on montmorillonite: Kinetic and equilibrium  
513 studies. *Colloids and Surfaces A: Physicochem. Eng. Aspects.* 449, 121–128.

514 Martín, J., Orta, M.M., Medina-Carrasco, S., Santos, J.L., Aparicio, I., Alonso, E.,  
515 2018. Removal of priority and emerging pollutants from aqueous media by  
516 adsorption onto synthetic organo-functionalized high-charge swelling micas.  
517 *Environ. Res.* 164, 488–494.

518 Martín, J., Orta, M.M., Medina-Carrasco, S., Santos, J.L., Aparicio, I., Alonso, E.,  
519 2019. Evaluation of a modified mica and montmorillonite for the adsorption of  
520 ibuprofen from aqueous media. *Appl. Clay Sci.* 171, 29-37.

521 Massarsky, A., Trudeau, V.L., Moon, T.W., 2011.  $\beta$ -blockers as endocrine disruptors:  
522 the potential effects of human  $\beta$ -blockers on aquatic organisms. *J. Exp. Zool. A*  
523 *Ecol. Genet. Physiol.* 315, 251–265.

524 Maszkowska, J., Stolte, S., Kumirska, J., Łukaszewicz, P., Mioduszevska, K.,  
525 Puckowski, A., Caban, M., Wagil, M., Stepnowski, P., Białk-Bielin ska, A., 2014.  
526 Beta-blockers in the environment: part I. mobility and hydrolysis study. *Sci. Total*  
527 *Environ.* 493, 1112-1121.

528 Mompelat, S., Le Bot, B., Thomas, O., 2009. Occurrence and fate of pharmaceutical  
529 products and by-products, from resource to drinking water. *Environ. Int.* 35, 803–  
530 814.

531 Orta, M.M., Martín J., Medina-Carrasco S., Santos J.L., Aparicio I., Alonso, E., 2018.  
532 Novel synthetic clays for the adsorption of surfactants from aqueous media. *J.*  
533 *Environ. Manag.* 206, 357-366.

534 Parolo, M.E., Avena, M.J., Savini, M.C., Baschini, M.T., Nicotra, V., 2013. Adsorption  
535 and circular dichroism of tetracycline on sodium and calcium-montmorillonites,  
536 *Colloids Surf. A* 417, 57–64.

537 Petrie, B., Barden, R., Kasprzyk-Hordern, B., 2015. A review on emerging  
538 contaminants in wastewaters and the environment: current knowledge,  
539 understudied areas and recommendations for future monitoring. *Water Res.* 72, 3-  
540 27.

541 Rauf, N., Tahir, S.S., Kang, J-H., Chang, Y-S., 2012. Equilibrium, thermodynamics and  
542 kinetics studies for the removal of alpha and beta endosulfan by adsorption onto  
543 bentonite clay, *Chem. Eng. J.* 192, 369–376.

544 Rodríguez-Narváez, O.M., Peralta-Hernandez, J.M., Goonetilleke, A., Bandala, E.R.,  
545 2017. Treatment technologies for emerging contaminants in water: A review.  
546 *Chem. Eng. J.* 323, 361–380.

547 Sánchez Martín, M.J., Sánchez Camazano, M., Hernández, M.T., Dominguez-Gil, A.,  
548 1981. Interaction of propranolol hydrochloride with montmorillonite. *J. Pharm.*  
549 *Pharmacol.* 33(6), 408-410.

550 Sannino, F., Violante, A., Gianfreda, L., 1997. Adsorption-desorption of 2,4-D by  
551 hydroxy aluminium montmorillonite complexes. *Pestic. Sci.* 51 (4), 429-435.

552 Santos, L.H.M.L.M., Gros, M., Rodriguez-Mozaz, S., Delerue-Matos, C., Pena, A.,  
553 Barceló, D., Montenegro, C.B.S.M., 2013. Contribution of hospital effluents to  
554 the load of pharmaceuticals in urban wastewaters: Identification of ecologically  
555 relevant pharmaceuticals. *Sci. Total Environ.* 461–462, 302–316.

556 Singh, N.B., Nagpal, G., Agrawal, S., Rachna., 2018. Water purification by using  
557 Adsorbents: A Review. *Environ. Technol. Innov.* 11, 187-240.

558 Smoluchowski, R., 1941. Anisotropy of the electronic work function of metals. *Phys.*  
559 *Rev.* 60, 661–674.

560 Soni, H., 2014. Martindale: the complete drug reference. *Emerg. Nurse.* 22 (5), 12.

561 Stanley, J.K., Ramirez, A.J., Mottaleb, M., Chambliss, C.K., Brooks, B.W., 2006.  
562 Enantiospecific toxicity of the  $\beta$ -blocker propranolol to *Daphnia magna* and  
563 *Pimephales promelas*. *Environ. Toxicol. Chem.* 25, 1780–1786.

564 Tarpani, R.R.Z., Azapagic, A., 2018. Life cycle environmental impacts of advanced  
565 wastewater treatment techniques for removal of pharmaceuticals and personal  
566 care products (PPCPs). *J. Environ. Manag.* 215, 258-272.

567 Ullah, H., Wahid, F., Santos, H.A., Khan, T. 2016. Advances in biomedical  
568 and pharmaceutical applications of functional bacterial cellulose-based  
569 nanocomposites. *Carb. Pol.* 150, 330-352.

570 Young, R.A. (Ed.), 1993. *The Rietveld Method*; IUCr Monographs on Crystallography  
571 No 5. Oxford University Press, New York.

572

573

574 **FIGURE CAPTION**

575 **Figure 1.** Experimental diffractograms obtained for Mt (black) and Mt after the  
576 adsorption assay of propranolol (red).

577 **Figure 2.** Thermal gravimetric analysis ((a) TG (b) DSC) before and after adsorption of  
578 propranolol onto Mt.

579 **Figure 3.** (a) Propranolol adsorption vs. equilibrium concentration, and (b) percentage  
580 of propranolol adsorption vs. initial concentration.

581 **Figure 4.** Langmuir, Freundlich and DR models of propranolol adsorption on Mt.

582 **Figure 5.** Kinetic models of propranolol adsorption on Mt.

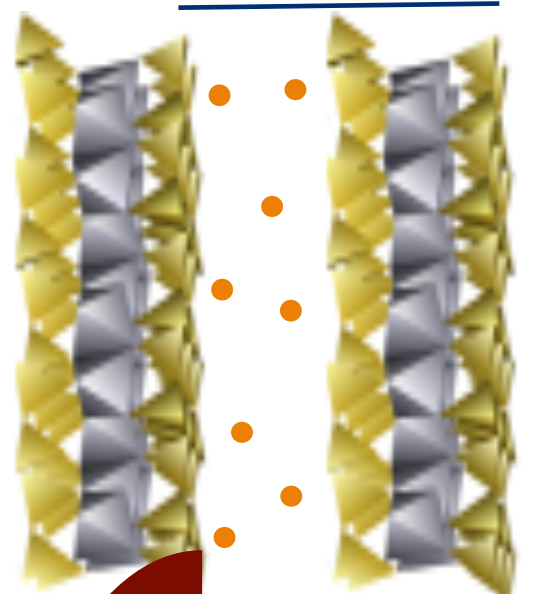


583 **Figure 6.** Effect of pH on propranolol adsorption on Mt.

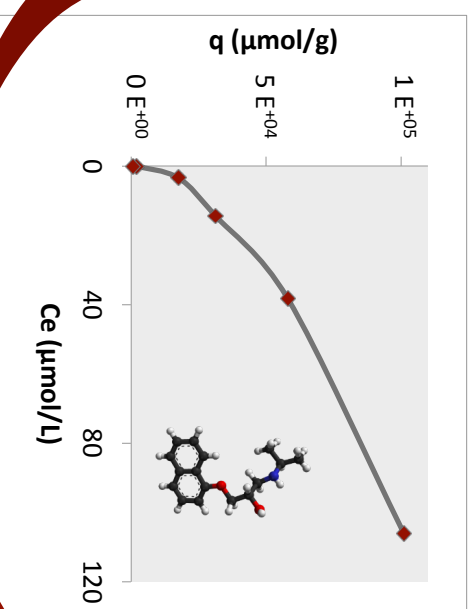
584

585

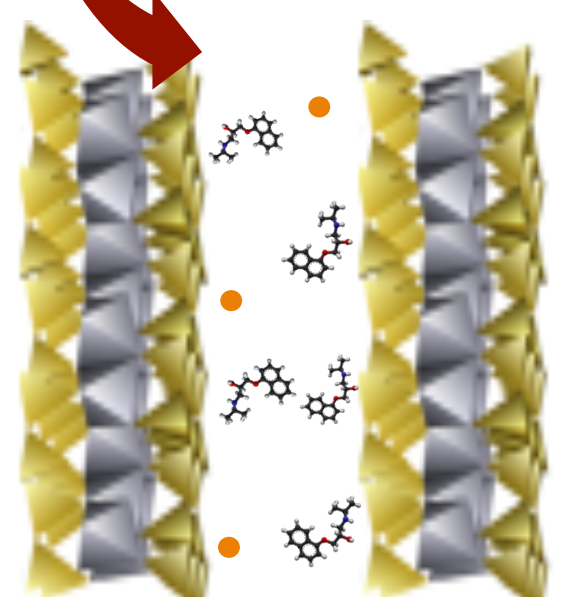
12.71 Å



Mt



13.45 Å



Mt-propranolol

## Highlights

- Mt represents a suitable adsorbent of propranolol from aqueous samples
- XRD and DSC-TG indicate that propranolol adsorption occurs in the interlayer space
- Propranolol adsorption is described by Freundlich and Dubinin-Radushkevitch models
- Exchange between propranolol and sodium in Mt interlayer is the pathway proposed
- After 1 min propranolol is 96% removed which is an extremely rapid kinetic behavior

**Table 1.** Langmuir, Freundlich and Dubinin-Radushkevitch parameters for propranolol adsorption on Mt.

Model	Parameter	Mt
Langmuir	$q_{\max}$ ( $\mu\text{mol/g}$ )	$1.1\text{E}^{+05}$
	$K_L$ ( $\text{L}/\mu\text{mol}$ )	0.05
	$R^2$	0.8947
	$\Delta q$ (%)	47.7
Freundlich	$K_F$ ( $\text{L/g}$ )	$6.5\text{E}^{+03}$
	$1/n$	0.61
	$R^2$	0.9932
	$\Delta q$ (%)	15.0
Dubinin-Radushkevitch	$q_{\max}$ ( $\mu\text{mol/g}$ )	$6.2\text{E}^{+05}$
	KDR ( $\text{mol}^2/\text{J}$ )	$3.7\text{E}^{-09}$
	E ( $\text{KJ/mol}$ )	11.6
	$R^2$	0.9973
	$\Delta q$ (%)	8.0

**Table 2.** Kinetic parameters of propranolol adsorption on Mt.

<b>Model</b>	<b>Parameter</b>	<b>Mt</b>
<b>PFO</b>	$q_e$ ( $\mu\text{mol/g}$ )	$8.86 \pm 0.01$
	$q_e$ cal ( $\mu\text{mol/g}$ )	$0.06 \pm 0.01$
	$k_1$ (1/min)	$0.25 \pm 0.05$
	$R^2$	0.9053
	$\Delta q$ (%)	61.9
<b>PSO</b>	$q_e$ cal ( $\mu\text{mol/g}$ )	$8.84 \pm 0.01$
	$k_2$ ( $\text{g}/\mu\text{mol}\cdot\text{min}$ )	$57.7 \pm 16.9$
	$R^2$	1.0000
	$\Delta q$ (%)	0.5
<b>IDM</b>	$k_i$ ( $\mu\text{mol}/\text{g}\cdot\text{min}^{1/2}$ )	$0.026 \pm 0.005$
	$C$ ( $\mu\text{mol/g}$ )	$8.78 \pm 0.01$
	$R^2$	0.8898
	$\Delta q$ (%)	0.1
<b>Elovich</b>	$\alpha$ ( $\mu\text{mol}/\text{g}\cdot\text{min}$ )	$3.7\text{E}^{272} \pm 1.0\text{E}^{272}$
	$\beta$ ( $\text{g}/\mu\text{mol}$ )	$71.1 \pm 5.28$
	$R^2$	0.9837
	$\Delta q$ (%)	0.0

Figure  
[Click here to download Figure: Revised Figure 1.PDF](#)

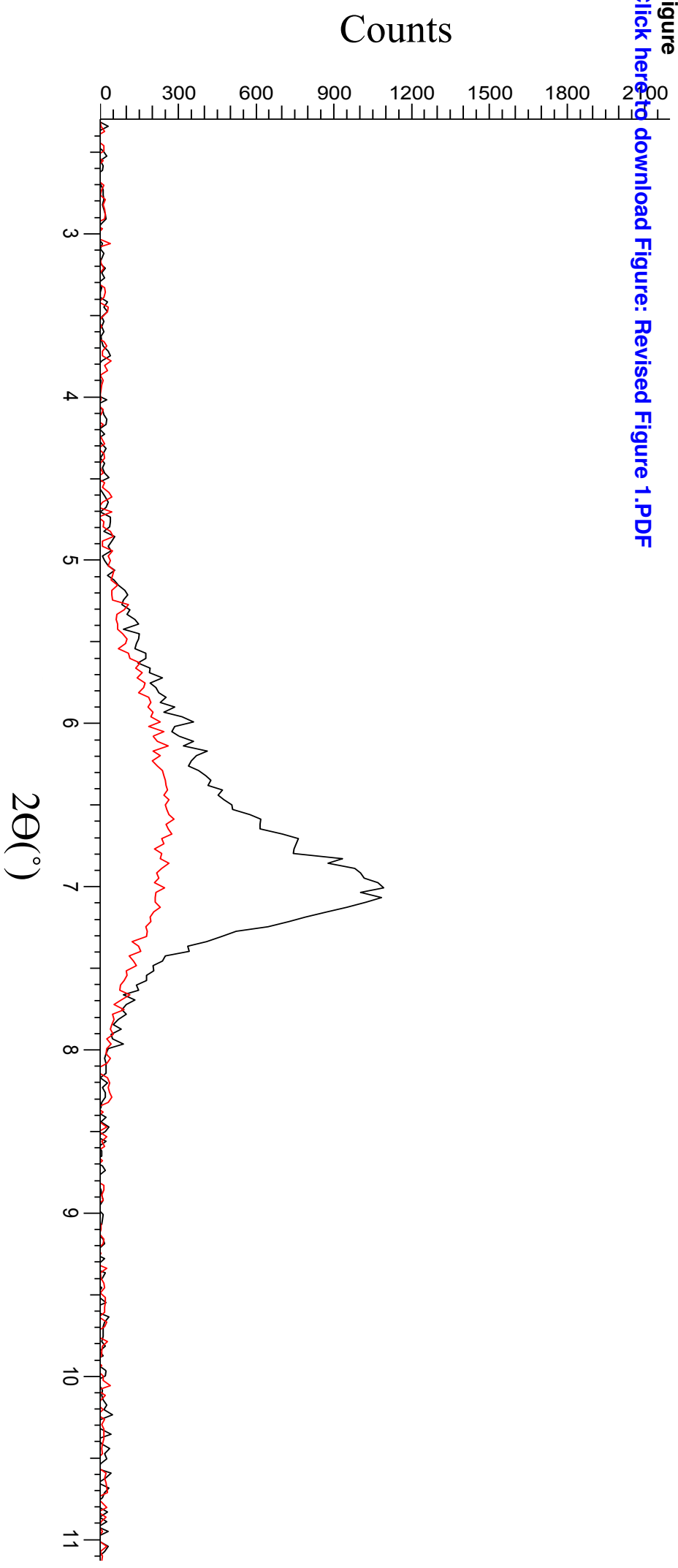
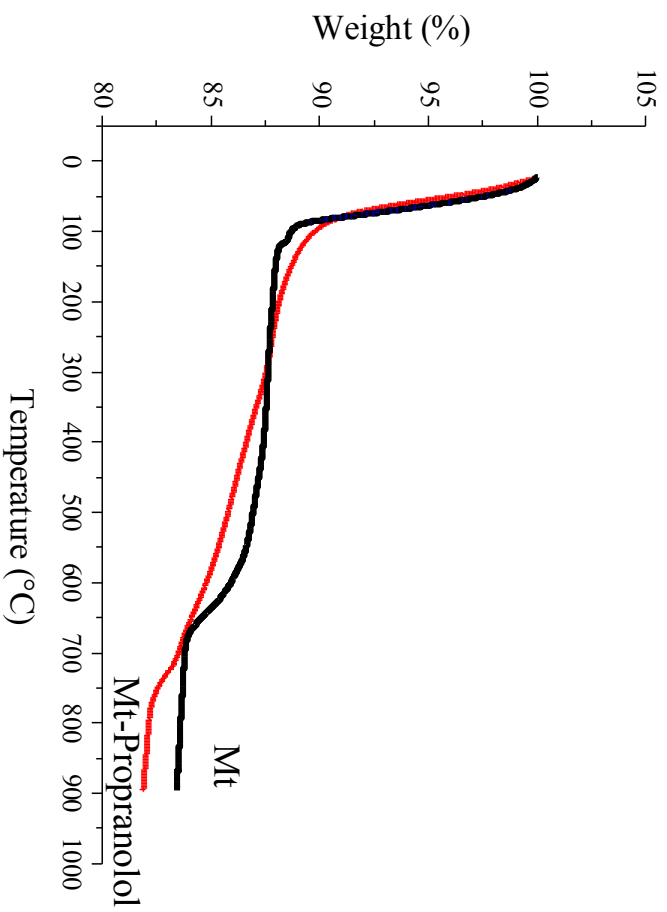
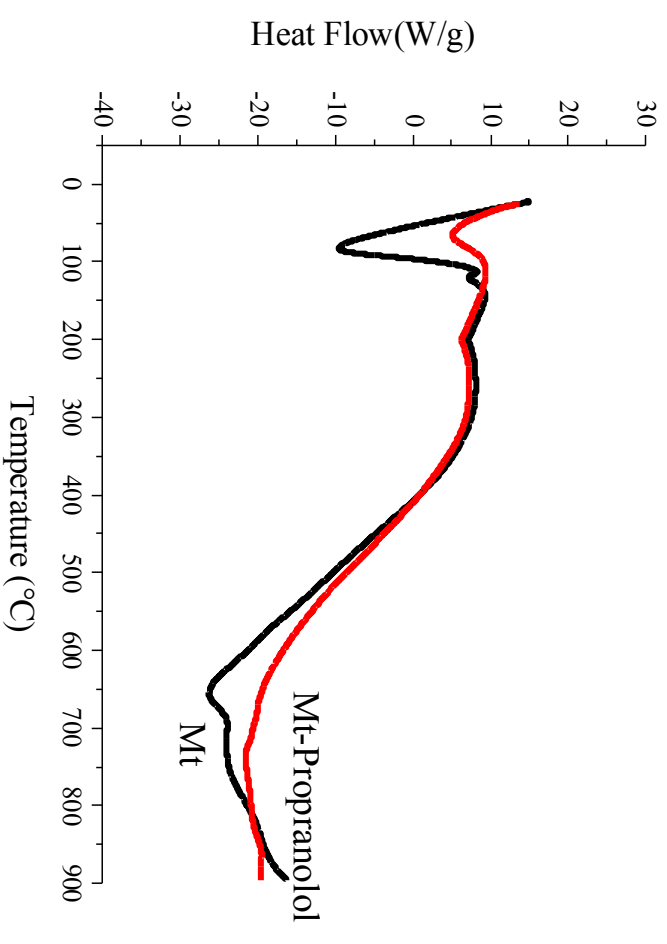


**Figure**  
[Click here to download Figure: Revised Figure 2.pdf](#)  
a)



b)



Figure

[Click here to download Figure: Revised Figure 3.pdf](#)

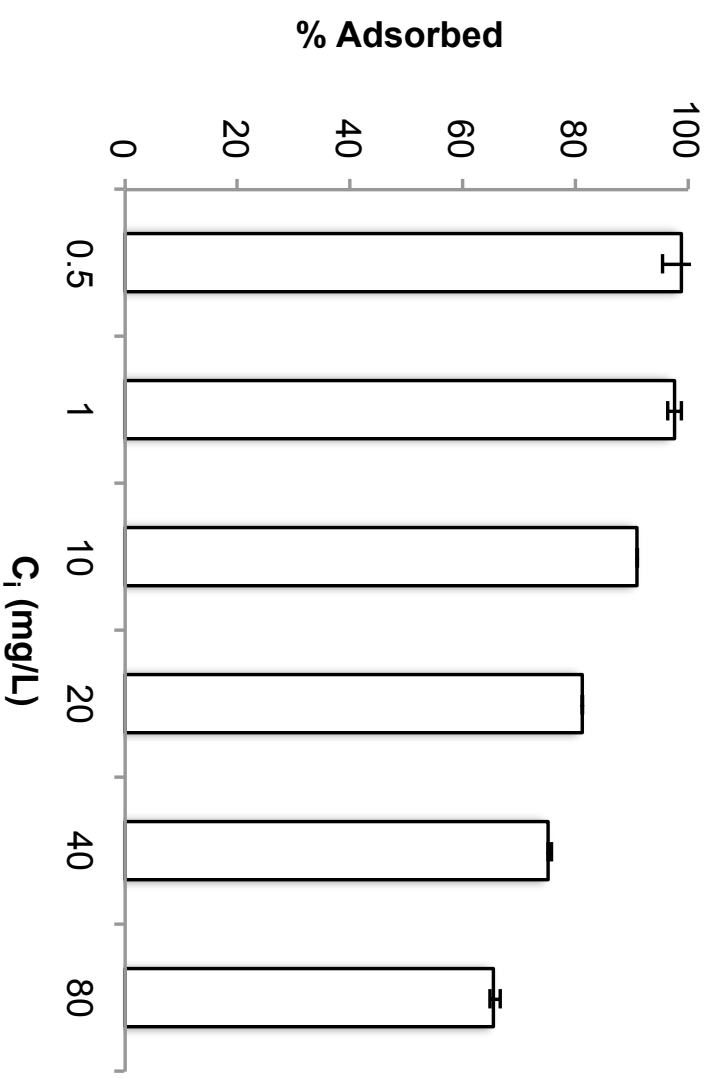
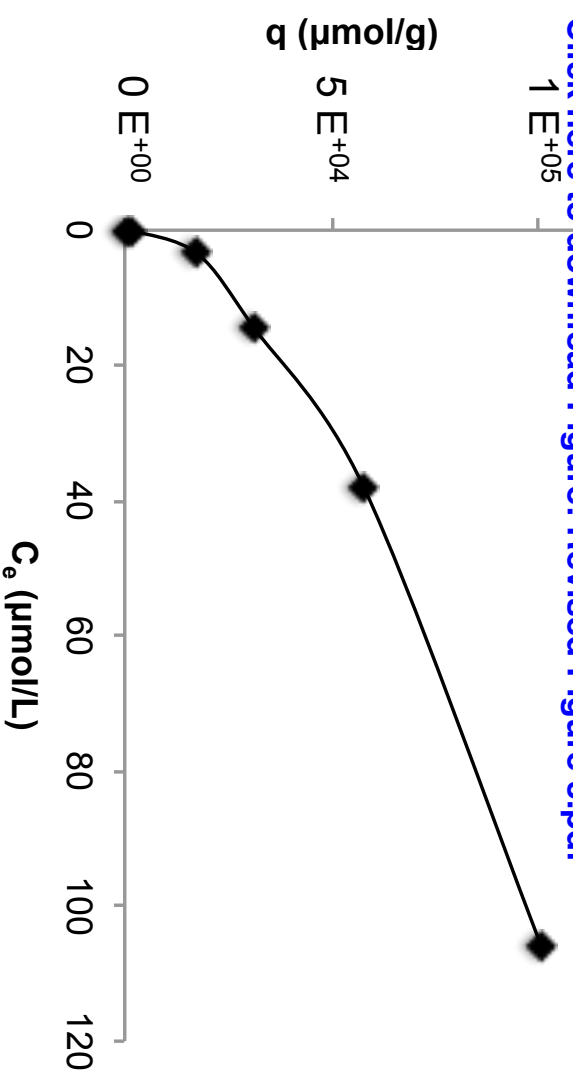




Figure 2

[Click here to download Figure: Revised Figure 4.pdf](#)

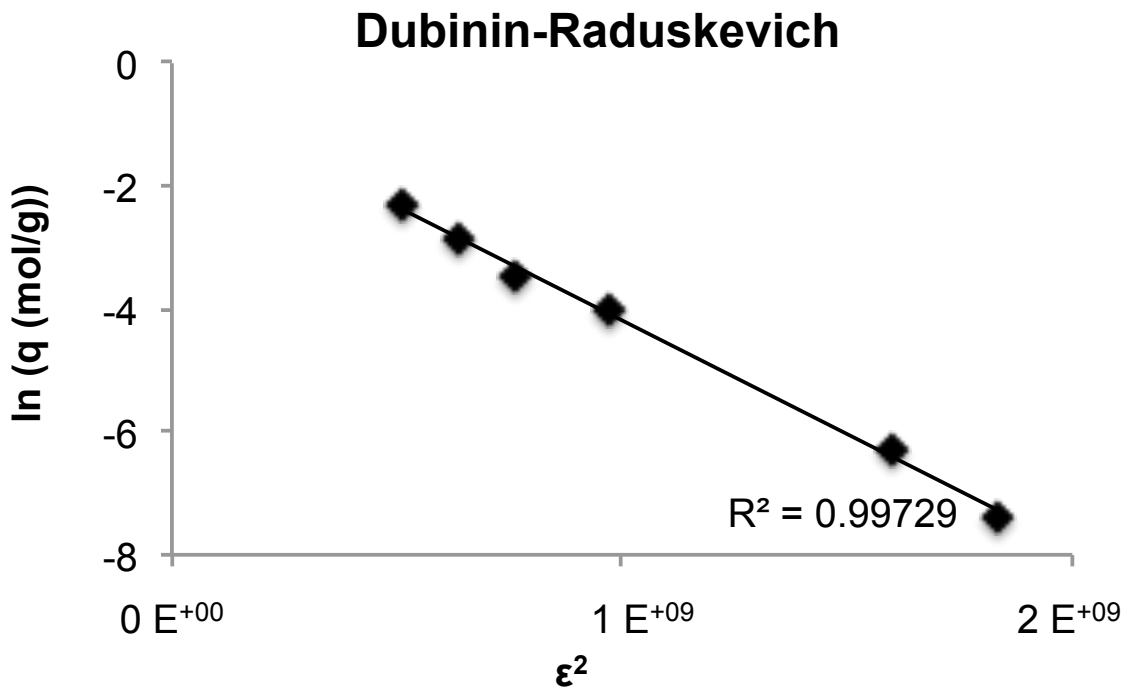
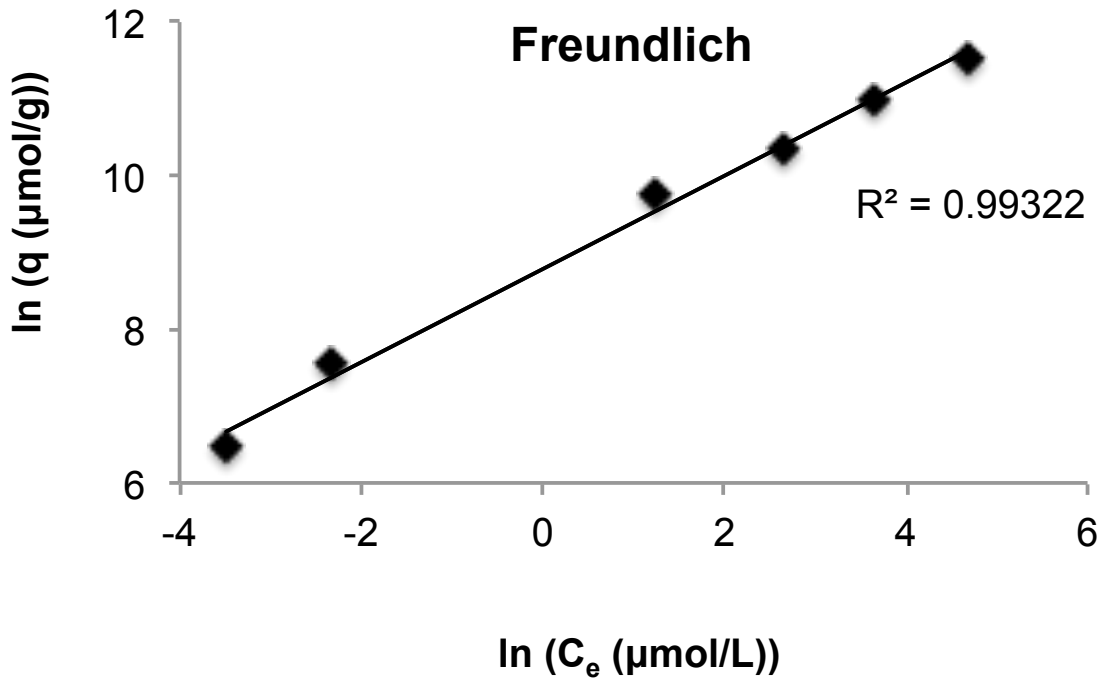
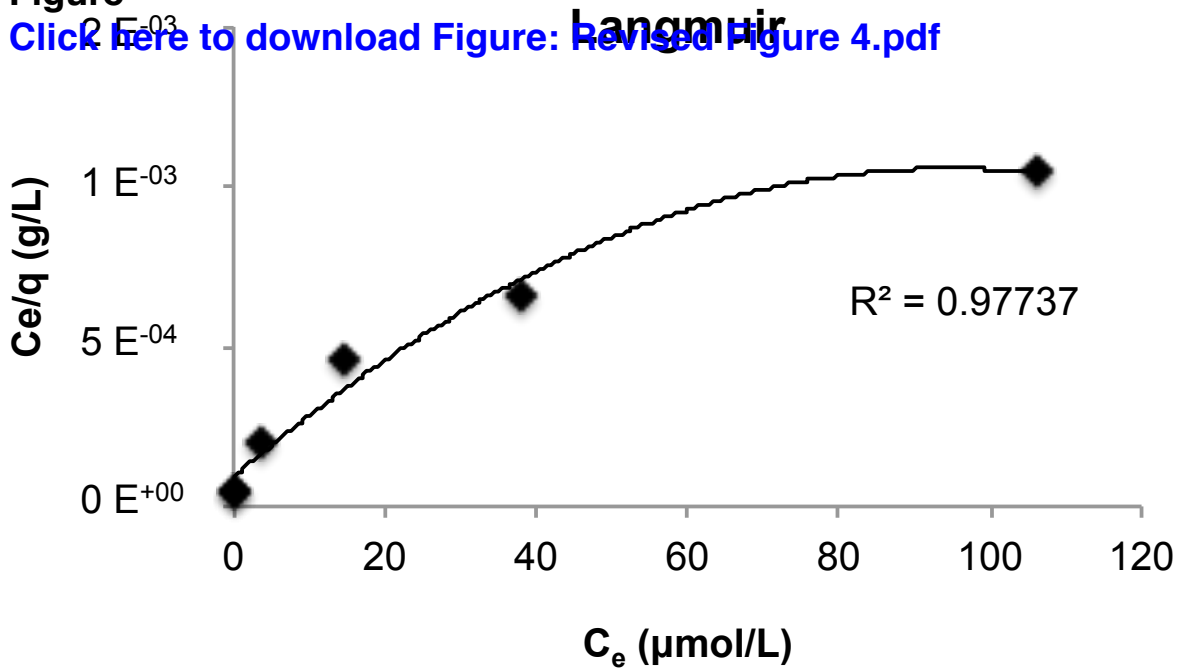
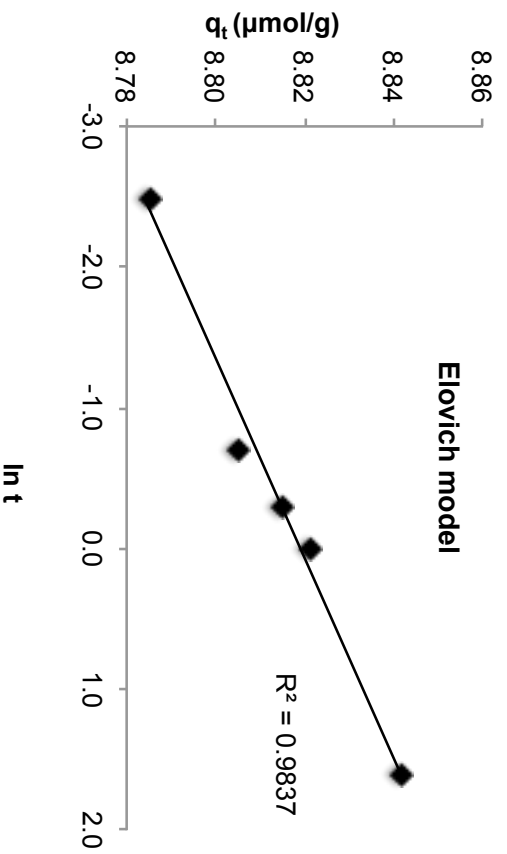
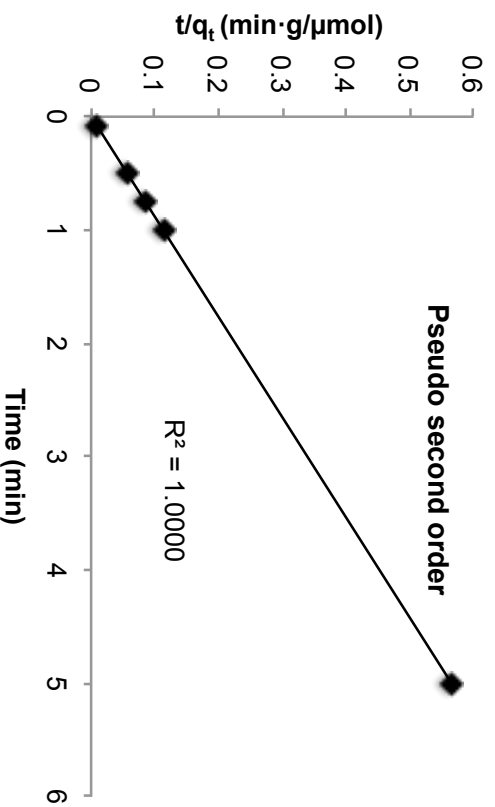
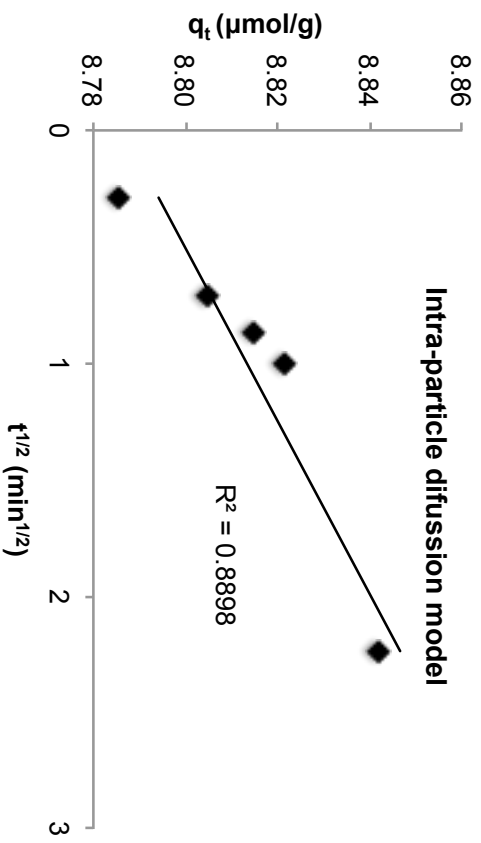
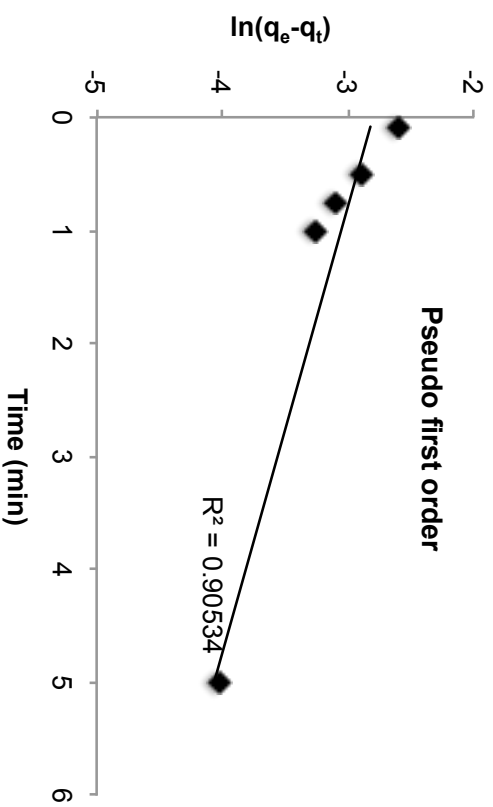
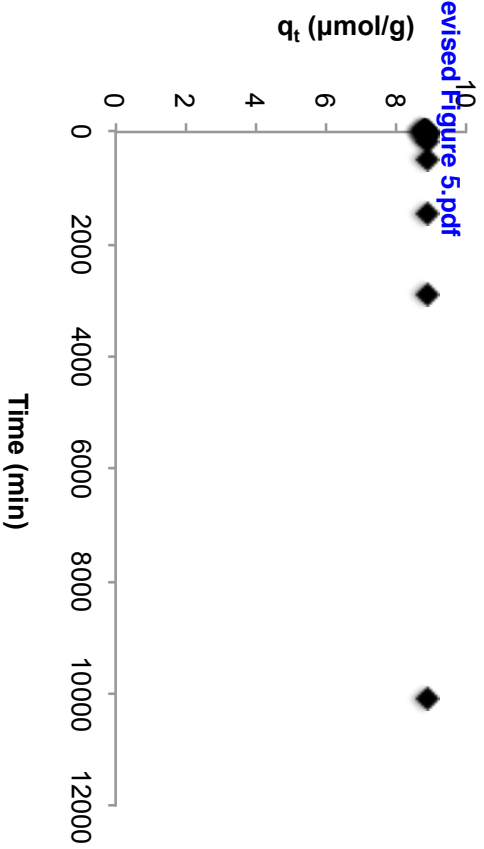


Figure  
[Click here to download Figure: Revised Figure 5.pdf](#)



Figure

[Click here to download Figure: Revised Figure 6.pdf](#)

